

Ramifications of the Nuclear Symmetry Energy for Neutron Stars, Nuclei, and Heavy-Ion Collisions

A. W. Steiner

*Joint Institute for Nuclear Astrophysics, National Superconducting
Cyclotron Laboratory, and the Department of Physics and Astronomy,
Michigan State University, East Lansing, MI 48824-2320*

B.-A. Li

*Department of Physics, Texas A&M University-Commerce
Commerce, TX 75429-3011*

M. Prakash

*Department of Physics and Astronomy, Ohio University
Athens, OH 45701-2979*

The pervasive role of the nuclear symmetry energy in establishing some nuclear static and dynamical properties, and in governing some attributes of neutron star properties is highlighted.

Keywords: Symmetry energy; Nuclear matter; Nuclei; Neutron stars; intermediate-energy heavy-ion collisions

1. Introduction

The nuclear symmetry energy, $E_s = \frac{1}{2} \frac{\partial^2 E}{\partial \delta^2}$, where $\delta = (n_n - n_p)/(n = n_n + n_p)$ with n_n and n_p denoting the neutron and proton densities and $E \equiv E(n, \delta)$ is the energy per particle, measures the stiffness encountered in making a system of nucleons isospin-asymmetric. Figure 1 schematically shows how the symmetry energy connects several nuclear and astrophysical observables. The difference between the energy per baryon of pure neutron matter and that of symmetric nuclear matter (containing equal numbers of neutrons and protons) at any particular density is largely given by the density dependent symmetry energy. Below, we highlight some recent work that has shed light on some of the connections between the symmetry energy and data from terrestrial experiments and astrophysical observations.

2. The Skin Thicknesses of Heavy Nuclei

Traditionally, constraints on the nuclear symmetry energy have been derived from mass measurements of nuclei. For neutron star physics, the correlation that exists^{2,3}

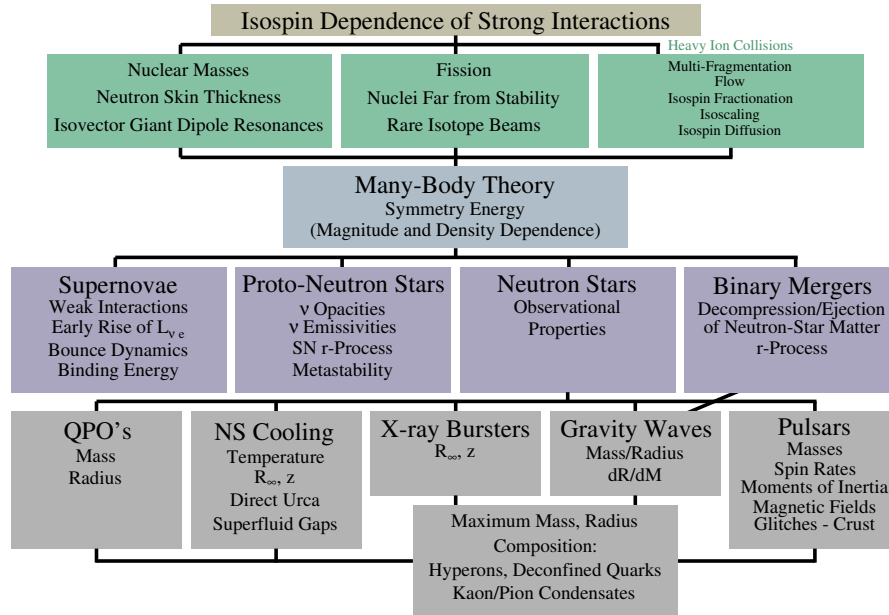


Fig. 1. The nuclear physics observables (top panels) and astrophysical observables (lower panels) are both connected to the nuclear symmetry energy, which is determined from nuclear many-body physics (adapted from Ref. 1).

between the neutron skin thicknesses in heavy nuclei, δR (the difference between the neutron and proton root-mean-square radii), and the pressure P of pure neutron matter at a density of $n \simeq 0.1 \text{ fm}^{-3}$ is particularly useful. Accurate measurements of δR can establish an empirical calibration point for the pressure of neutron star matter at subnuclear densities. The connection between the neutron skin thickness and the symmetry energy has been known from Bodmer's work in the 60's.⁴ The Typel-Brown correlation between δR and $P(5n_0/8)$, which is closely related to the density derivative of the symmetry energy, demonstrates clearly the new information that could be obtained by accurate measurements of skin thicknesses in heavy nuclei. Figure 2 shows the correlation between the skin thickness δR of ^{208}Pb and the pressure of beta-equilibrated matter at 0.1 fm^{-3} for several potential models (based on the Skyrme interaction) and field-theoretical models.¹ The skin thickness of ^{208}Pb is scheduled to be measured at the Jefferson Lab in the summer of 2008 in the PREX experiment^{5,6} and will likely provide a stringent constraint.

3. Intermediate-Energy Heavy-Ion Collisions

The possibility of determining the equation of state (EOS) of nucleonic matter from heavy-ion collisions has been discussed for almost 30 years. A number of heavy-ion collision probes of the symmetry energy have been proposed including isospin fractionation,^{7,8} isoscaling,^{9,10} neutron-proton differential collective flow,¹¹ pion pro-

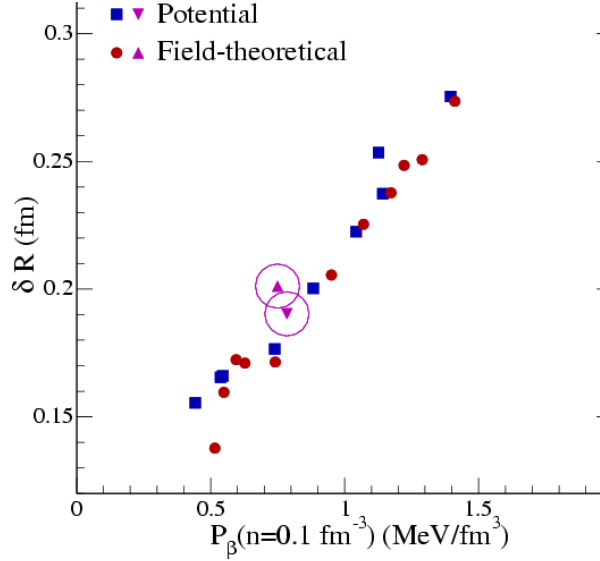


Fig. 2. The correlation between neutron skin thickness of ^{208}Pb and the pressure of neutron star matter for the models described in Ref. 1.

duction,¹² isospin diffusion,¹³ and neutron-proton correlation functions.¹⁴ Determination of the EOS from heavy-ion data involves comparisons of transport model simulations^{15–17} with experimental data given an input EOS. Transport model simulations track the evolution of the phase space distribution function (not necessarily that of an equilibrium distribution function at finite temperature) at momenta that usually exceed those found in the static initial configurations. As the driving force is the density functional derivative of the energy density (the in-medium cross sections control the collision integral), access to the cold EOS at high densities is afforded.

Isospin diffusion is caused by the exchange of neutrons and protons between nuclei in a heavy-ion collision (Fig. 3). This diffusion process, driven by the symmetry energy, moves the target and projectile nuclei toward isospin symmetry. To gain access to details of the diffusion process, fragment emission during and after the collision must be taken into account. This requirement is achieved by considering the ratio¹⁸

$$R_\delta = \frac{2\delta^{A+B} - \delta^{A+A} - \delta^{B+B}}{\delta^{A+A} - \delta^{B+B}}, \quad (1)$$

where A and B denote nuclei with different isospin asymmetries and δ is the isospin asymmetry of the projectile-like fragment.

Recently, isospin diffusion has been exploited to constrain the symmetry energy from reactions involving ^{112}Sn and ^{124}Sn at the NSCL,^{13,20} leading to $R_\delta \sim 0.46$. In conjunction with an isospin- and momentum-dependent transport model, IBUU04,^{21,22} the NSCL data on isospin diffusion can be used to constrain the symmetry energy. Writing the symmetry energy in terms of a kinetic part and a potential

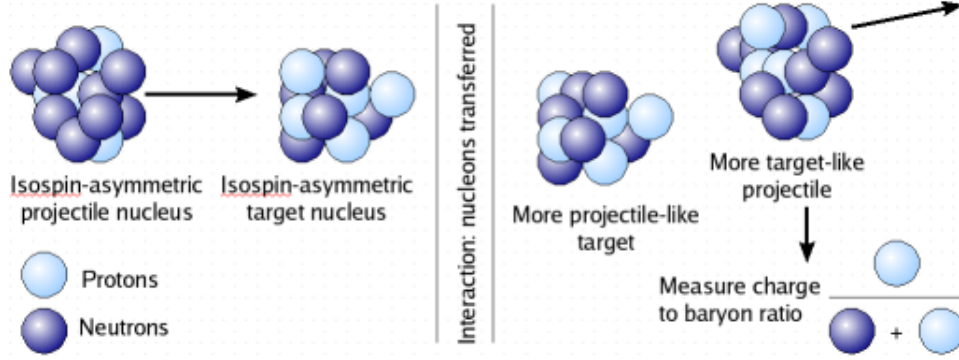


Fig. 3. Isospin diffusion process during a heavy-ion collision (from Ref. 19).

part as

$$E_s(n) = S_v(n/n_0)^\gamma, \quad (2)$$

where S_v is the symmetry energy at the nuclear equilibrium density, $n_0 = 0.16 \text{ fm}^{-3}$, the constraint $0.69 < \gamma < 1.05$ has been found.^{20,23} This constraint is consistent with the symmetry energy inherent in the EOS (computed using Monte Carlo simulations with input two- and three-body interactions which are matched to nucleon-nucleon scattering phase shifts and the energy levels of light nuclei) of Akmal, et al.²⁴ (APR). This constraint also rules out models with values of $\gamma > 1.05$ found in some field-theoretical models.

Because intermediate-energy heavy-ion collisions provide a constraint on the symmetry energy at the same densities as would be probed by a measurement of the neutron skin thickness of ^{208}Pb , the NSCL data also provides a restrictive range for its neutron skin thickness. This connection was used in Refs. 25 and 23 to show that the neutron skin thickness of ^{208}Pb should be at least greater than 0.15 fm in order to be consistent with the NSCL data, with values between 0.23 fm and 0.27 fm favored by the transport model simulations (Fig. 4).

4. Neutron Star Radii

Neutron star radii tend to probe the density dependence of the symmetry energy around the nuclear equilibrium density, $n_0 = 0.16 \text{ fm}^{-3}$. Lattimer and Prakash²⁶ found that the radius R of a neutron star exhibits the power law correlation:

$$R \simeq C(n, M) [P(n)]^{0.23-0.26}, \quad (3)$$

where $P(n)$ is the total pressure inclusive of leptonic contributions evaluated at a density n in the range n_0 to $2n_0$, and $C(n, M)$ is a number that depends on the density n at which the pressure is evaluated and on the stellar mass M . The left panel in Fig. 5 shows this correlation as $RP^{-\alpha}$ versus R for stars of mass

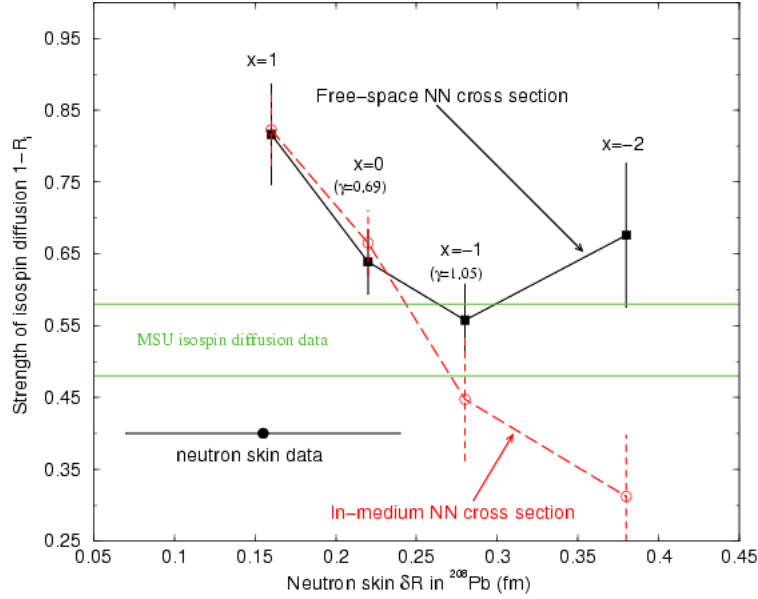


Fig. 4. The correlation between the neutron skin thickness and the amount of isospin diffusion in collisions between Sn isotopes as measured at the NSCL (from Ref. 23).

$1.4 M_{\odot}$. Neutron star radius measurements, especially those with uncertainties less than about 0.5 km, constrain the symmetry energy above the nuclear equilibrium density. These constraints will be much improved when simultaneous mass and radius measurements of the same object become available.

If there is no phase transition between n_0 and a few times n_0 , the range in which neutron star radii are determined mainly by the symmetry energy, results from the isospin diffusion data at the NSCL can be used to constrain neutron star radii.²⁷ As only EOSs with symmetry energies between $x = 0$ and $x = -1$ (where x is a parameter designed to vary the density dependence of the symmetry energy without modifying the magnitude of the symmetry energy at n_0 or the isospin-symmetric part of the EOS) are consistent with the isospin diffusion data, this range of x values is representative of the possible variation in neutron star structure that is consistent with terrestrial data. Neutron star radii, while being strong functions of the symmetry energy, are also affected by contributions from the isospin-symmetric part of the EOS, especially at high densities. About 5% difference is representative of the radius uncertainty stemming from the symmetric part of the EOS. The conclusion of Ref. 27 is that only radii between 11.5 and 13.6 km (or radiation radii between 14.4 and 16.3 km) are consistent with the $x = 0$ and $x = -1$ EOSs (see the right panel in Fig. 5).

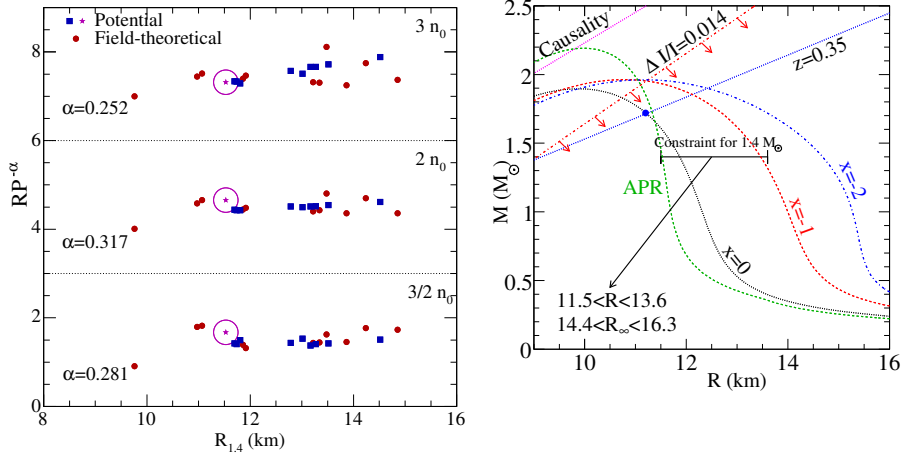


Fig. 5. (Left) The value $RP^{-\alpha}$ for several field-theoretical and potential models considered in Ref. 1. The values of α correspond to the density indicated in the upper right corner of each block. (Right) The constraint on the radius of 1.4 solar mass neutron stars as determined from isospin diffusion in heavy-ion collisions (from Ref. 27).

5. The Direct Urca Process

The long-term cooling of a neutron star is chiefly determined by its composition. Beta equilibrium and charge neutrality determine the proton fraction in neutron-star matter and thus the critical density for the onset of the direct Urca processes $n \rightarrow p + e + \bar{\nu}$ and $e + p \rightarrow n + \nu$, which cool the star more rapidly than the modified Urca processes in which an additional nucleon is present.²⁸ The direct Urca processes, however, require a sufficient amount of protons in matter (of order 10-14%).

Larger symmetry energies induce larger proton fractions (with matter being closer to isospin-symmetric) and smaller critical densities for the onset of the direct Urca processes. However, higher than quadratic terms in the energy $E(n, \delta)$ of isospin asymmetric matter can have an important role to play.²⁹ Recently, Steiner³⁰ has shown that quartic terms in $E(n, \delta)$ play an important role in determining the critical density for the direct Urca process. Such terms can be easily generated within the context of field-theoretical models. This is demonstrated in Fig. 6 for the Akmal, et al., (1998) EOS, for which the relative size of the quartic and quadratic terms is parametrized by η as described in Ref. 30. The mass and radius are virtually unchanged, whereas the threshold density for the direct Urca process changes by more than a factor of two.

Gusakov, et al.,³¹ have investigated the cooling of neutron stars using the EOS of APR.²⁴ They found that, because of the direct Urca process, stars with masses

larger than about $1.7 M_{\odot}$ cool so rapidly as to be cooler than nearly all of the observed neutron stars. Our work offers a possible resolution: quartic terms can play a role at high density to turn off the direct Urca process thus making the computed cooling curves match the comparatively warm neutron stars.

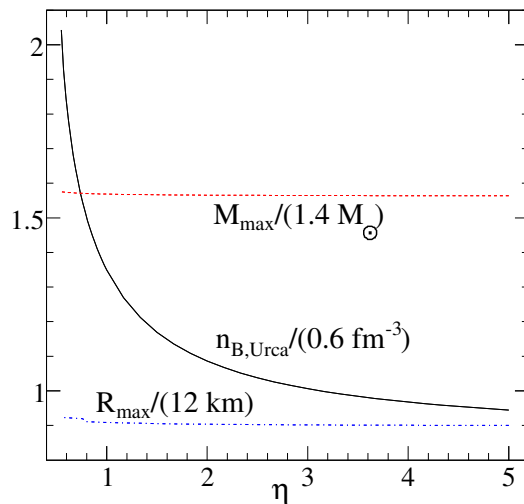


Fig. 6. The maximum mass, the radius of the maximum mass star, and the critical density for the direct Urca process as a function of η , which describes the strength of quartic terms in the symmetry energy (from Ref. 30).

6. Outlook

In addition to the role of the symmetry energy in the few areas highlighted here, its importance in controlling the cooling times of transient x-ray bursters, seismic activity of neutron star surfaces, ejection of baryons during binary mergers, etc., is only beginning to be appreciated. The PREX experiment, heavy-ion experiments, neutron star mass, radius and surface temperature measurements, observations of transient x-ray bursters etc., all hold keys to pin down the magnitude and density dependence of the symmetry energy in addition to delineating its pervasive role.

7. Acknowledgments

Research support for A. W. S. by the Joint Institute for Nuclear Astrophysics under the NSF-PFC grant PHY 02-16783, for B-A. L. in parts by the NSF under Grant No. PHY0652548 and the Research Corporation under Award No. 7123, and for M. P. by the DOE under Grant. DE-FG02-93ER40756 is gratefully acknowledged.

References

1. A. W. Steiner, M. Prakash, J. M. Lattimer and P. J. Ellis, *Phys. Rep.* **411**, p. 325 (2005).
2. B. A. Brown, *Phys. Rev. Lett.* **85**, p. 5296 (2000).
3. S. Typel and B. A. Brown, *Phys. Rev. C* **64**, p. 027302 (2001).
4. A. R. Bodmer, *Nucl. Phys.* **17**, p. 388 (1960).
5. R. Michaels, P. A. Souder and G. M. Urciuoli, *Jefferson Laboratory Proposal PR-00-003* (2000).
6. C. J. Horowitz, S. J. Pollock, P. A. Souder and R. Michaels, *Phys. Rev. C* **63**, p. 025501 (2001).
7. H. Muller and B. Serot, *Phys. Rev. C* **52**, p. 2072 (1995).
8. B. A. Li and C. M. Ko, *Nucl. Phys. A* **618**, p. 498 (1997).
9. M. B. Tsang, W. A. Friedman, C. K. Gelbke, W. G. Lynch, G. Verde and H. S. Xu, *Phys. Rev. Lett.* **86**, p. 5023 (2001).
10. A. Ono, P. Danielewicz, W. A. Friedman, W. G. Lynch and M. B. Tsang, *Phys. Rev. C* **68**, p. 051601(R) (2003).
11. B.-A. Li, *Phys. Rev. Lett.* **85**, p. 4221 (2000).
12. B.-A. Li, *Phys. Rev. Lett.* **88**, p. 192701 (2002).
13. M. B. Tsang, T. X. Liu, L. Shi, P. Danielewicz, C. K. Gelbke, X. D. Liu, W. G. Lynch, W. P. Tan, G. Verde, A. Wagner, H. S. Xu, W. A. Friedman, L. Beaulieu, B. Davin, R. T. de Souza, Y. Larochele, T. Lefort, R. Yanez, V. E. Viola, Jr., R. J. Charity and S. L. G., *Phys. Rev. Lett.* **92**, p. 062701 (2004).
14. L.-W. Chen, V. Greco, C. M. Ko. and B.-A. Li, *Phys. Rev. Lett.* **90**, p. 162701 (2003).
15. B.-A. Li, C. M. Ko and W. Bauer, *Int. Jour. Mod. Phys. E* **7**, p. 147 (1998).
16. B.-A. Li and W. U. Schröder (eds.), *Isospin Physics in Heavy-Ion Collisions at Intermediate Energies* (Nova Science Publishers, Inc., New York, 2001).
17. P. Danielewicz, R. Lacey and W. G. Lynch, *Science* **298**, p. 1592 (2002).
18. F. Rami, Y. Leifels, B. de Schauenburg, A. Gobbi, B. Hong, J. P. Alard, A. Andronic, R. Averbeck, V. Barret, Z. Basrak, N. Bastid, I. Belyaev, A. Bendarag and G. Berek, *Phys. Rev. Lett.* **84**, p. 1120 (2000).
19. J. M. Lattimer and M. Prakash, *Phys. Rep.* **442**, p. 109 (2006).
20. L.-W. Chen, C. M. Ko and B.-A. Li, *Phys. Rev. Lett.* **94**, p. 032701 (2005).
21. B.-A. Li, C. B. Das, S. Das Gupta and C. Gale, *Phys. Rev. C* **69**, p. 011603(R) (2004).
22. B.-A. Li, C. B. Das, S. Das Gupta and C. Gale, *Nucl. Phys. A* **735**, p. 563 (2004).
23. B.-A. Li and L.-W. Chen, *Phys. Rev. C* **72**, p. 064611 (2005).
24. A. Akmal, V. R. Pandharipande and D. G. Ravenhall, *Phys. Rev. C* **58**, p. 1804 (1998).
25. A. W. Steiner and B.-A. Li, *Phys. Rev. C* **72**, p. 041601 (2005).
26. J. M. Lattimer and M. Prakash, *Astrophys. J.* **550**, p. 426 (2001).
27. B.-A. Li and A. W. Steiner, *Phys. Lett. B* **642**, 436 (2006).
28. J. M. Lattimer, C. J. Pethick, M. Prakash and P. Haensel, *Phys. Rev. Lett.* **66**, p. 2701 (1991).
29. H. Muether, M. Prakash and T. L. Ainsworth, *Phys. Lett. B* **199**, p. 469 (1988).
30. A. W. Steiner, *Phys. Rev. C* **74**, p. 045808 (2006).
31. M. E. Gusakov, A. D. Kaminker, D. G. Yakovlev and O. Y. Gnedin, *Mon. Not. R. Astron. Soc.* **363**, p. 555 (2005).